Single Pole-Double Throw (Reciprocal)

If it is desired to produce reciprocal single pole-double throw action, this can be done efficiently by using one nonreciprocal switchable circulator and two fixed circulators as shown in Fig. 5.

The action of the switch can be seen by following the path of the power flow. Power enters SW_1 and proceeds in the sense of the solid arrow through C_1 to Load 1. Power returned from Load 1 proceeds through C_2 and SW_1 back to the input. When SW_1 is switched so that the dashed arrow applies, power entering at the input proceeds through C_2 to Load 2. Power returned from Load 2 travels to C_1 and then to SW_1 and back to the input. This switch then produces reciprocal power flow. The forward- and reverse-phase in this switch may be different although it could be adjusted by choosing proper line lengths. The insertion loss in the two directions are not equal since, in the forward direction one suffers the loss of two circulators, while in the reverse direction the loss is due to passing through three circulators.

A reciprocal single-pole N-throw switch can be obtained by combining single pole-double throw switches, either in a parallel or series arrangement. A series arrangement is shown in Fig 6.

Double Pole-Double Throw (Nonreciprocal)

A nonreciprocal double pole-double throw switch can be designed using two switchable junction circulators. This circuit is shown in Fig. 7. When the two switches are electrically ganged together, the switching action can be seen as follows. First, when the solid arrow applies, In_1 is connected to Out_1 and In_2 is connected to Out_2 by the energy passing directly through SW_1 and SW_2, respectively. When the circulators are switched and the dashed arrows apply, In_1 is connected to Out_2 by energy passing through both SW_1 and SW_2. Similarly. In_2 is connected to Out_1. The switch is nonreciprocal since the following sequences apply.

Solid Arrow	Dashed Arrow
$In_1 \rightarrow Out_1$	$In_1 \rightarrow Out_2$
$In_2 \rightarrow Out_2$	$In_2 \rightarrow Out_1$
$Out_1 \rightarrow In_2$	$Out_1 \rightarrow In_1$
$Out_2 \rightarrow In_1$	$Out_2 \rightarrow In_2$

Double Pole-Double Throw (Reciprocal)

The switch of Fig. 8 can be made reciprocal by the addition of two circulators as shown schematically in Fig. 8.

The reader can verify that the following switching sequences take place.

Solid Arrow	Dashed Arrow
$In_1 \rightarrow Out_1$	$In_1 \rightarrow Out_2$
$In_2 \rightarrow Out_2$	$In_2 \rightarrow Out_1$
$Out_1 \rightarrow In_1$	$Out_1 \rightarrow In_2$
$Out_2 \rightarrow In_2$	$Out_2 \rightarrow In_1$

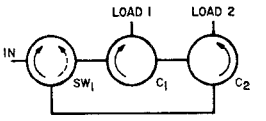

Fig. 5—Reciprocal single pole-double throw switch.

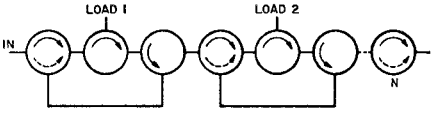

Fig. 6—Series arrangement of single pole-double throw reciprocal switches to make single pole-N throw switch.

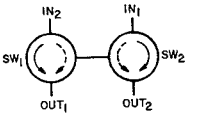

Fig. 7—Double pole-double throw nonreciprocal switch.

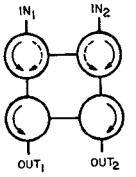

Fig. 8—Double pole-double throw reciprocal switch.

Experimental Characteristics

The three-port circulator shown in Fig. 2, having broad-band tuning, was investigated experimentally to observe its switching characteristics. The instantaneous bandwidth with a fixed field is shown in Fig. 9. The insertion loss vs coil current for several frequencies is shown in Fig. 10. An important characteristic should be noted from Fig. 10. It is difficult to overdrive this type of switch. The isolation and insertion loss show little change when one applies additional current to the unit. This is obviously not true in Faraday rotation switches, or switches utilizing phase shift principles. The fact that the switches are not current sensitive is an advantage to the systems engineer who need not worry about the design of a precision driver. Hysteresis measurements have shown this switch to have a maximum separation of 2 db between increasing and decreasing currents after driving the switch into saturation. Some of the hysteresis is due to the iron coil-forms used.

The coil current required is somewhat arbitrary and can be controlled by the number of turns and wire size. For fast switching requirements, inductance must also be controlled and some freedom of choice is lost. The holding power can be made extremely small by careful design. For example, a switch designed for space applications drew a current of 10 ma at 1 3/4 volts for proper operations.

Several arrangements for combining nonreciprocal, three-port switches with three-port circulators to produce reciprocal switches have been described. Single pole-single throw, single pole-double throw, double pole-double throw as well as balanced switches can be designed. These switches do not require exact values of switching current to obtain their best performance, and should find system use due to their small physical size. Some problems may be encountered with these devices due to their nonconstant input impedance during switching, as well as the difficulty in obtaining very rapid switching times.

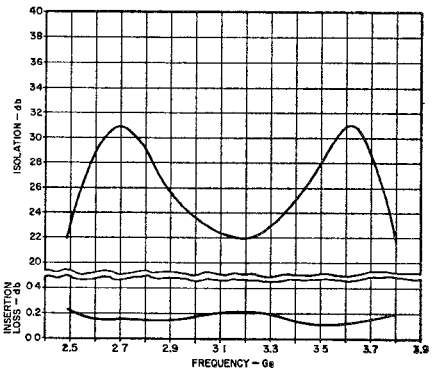

Fig. 9—Instantaneous isolation and insertion loss bandwidth of 3-port switchable junction circulator with fixed field.

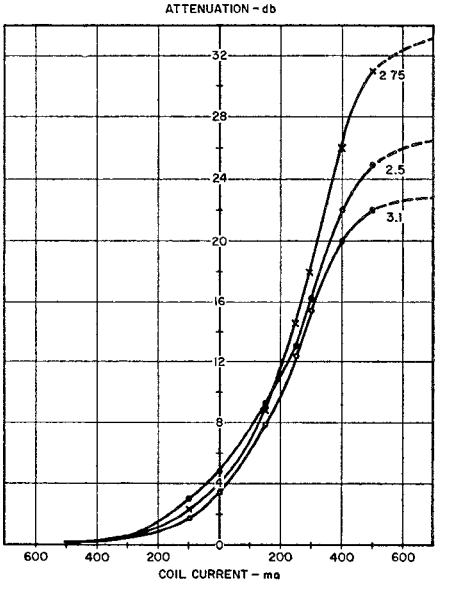

Fig. 10—Attenuation vs coil current for various frequencies for a switchable junction circulator. Only one-half of the frequency band is shown.

Alvin Clavin
RANTEC Corp.
Calabasas, Calif.

Mixed Two-Port Parameters for Characterizing Varactor Mounts in Waveguides*

In the design of harmonic generators using varactors in waveguide mounts, one of the most important problems is to determine

* Received November 7, 1962.

the impedance seen from the terminals of the nonlinear junction capacitance, as well as the transfer properties of the networks between the terminals of this capacitance and the output and input waveguides. Since the junction region in most cases of interest is many times smaller than one wavelength in size, the logical variables for describing the electrical conditions at the junction terminals are voltage and current. On the other hand, at the input and output waveguide ports, scattering variables a and b would be preferable. This communication will define a parameter system for two ports, where voltage and current are used as variables on one side, and scattering variables on the other. A method for experimental determination of these parameters will also be outlined.

When defining a new set of two-port parameters the notation problem immediately arises. Previously, the letters Z, Y, H, K, A and B have been used for the six possible permutations between two voltages V_1, V_2 and two currents, I_1 and I_2. For scattering variables, S and T (transmission matrix) have gained acceptance. The letter M will be used for the new matrix, one reason being the "mixed" character of the variables.

The notations used are shown in Fig. 1, and the equations read

$$b = m_{11}V + m_{12}I$$
$$a = m_{21}V + m_{22}I. \tag{1}$$

The dimension of m_{11} and m_{21} is $(\text{ohm})^{-1/2}$, for m_{12}, $m_{22}(\text{ohm})^{1/2}$.

In (1), four seemingly independent parameters are used to describe the two port. We know, however, that a passive and reciprocal two port can be described by only three independent parameters, and there must be some relationship between the m's appearing in (1).

There is one connecting link between the M matrix and the well-known S matrix, namely the case where the terminals 2 in Fig. 1 is terminated by a TEM-transmission-line (*e.g.*, a coaxial cable). On such a line, one can define voltage and current unambiguously as well as scattering variables a and b. Let us introduce the scattering variables a_2 and b_2 at port 2 in Fig. 1. If one assumes that V and I represent rms values of sinusoidal voltage and current, we get the following relationship between a_2, b_2, V and I:

$$V = \sqrt{Z_0}\,(a_2 + b_2)$$
$$I = \frac{a_2 - b_2}{\sqrt{Z_0}} \tag{2}$$

where Z_0 is the characteristic impedance of the TEM-line.

By inserting (2) into (1), and rearranging the equations to form a system of the well-known form

$$b_1 = s_{11}a_1 + s_{12}a_2$$
$$b_2 = s_{21}a_1 + s_{22}a_2 \tag{3}$$

one gets the desired relationship between the m's by setting $s_{12} = s_{21}$. The result is

$$|M| = m_{11}\cdot m_{22} - m_{12}\cdot m_{21} = -\tfrac{1}{2} \tag{4}$$

Fig. 1.

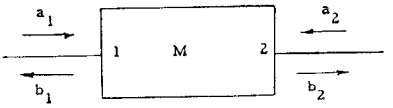

Fig. 2.

(independent of Z_0)

Two important expressions can now be written down in terms of the m's:

1) The input reflection coefficient in the waveguide $\Gamma_{in} = b/a$, when port 2 is terminated by an impedance $Z_T = -V/I$ ($m_{21} \neq 0$ is assumed)

$$\Gamma_{in} = \frac{m_{11}}{m_{21}} + \frac{1}{2(m_{21}\cdot m_{22} - Z_T m_{21}^2)}. \tag{5}$$

2) The input impedance $Z_{in} = V/I$, when the waveguide (port 1) is terminated with a reflection coefficient $\Gamma_T = a/b$

$$Z_{in} = -\frac{m_{22} - \Gamma_T m_{12}}{m_{21} - \Gamma_T m_{11}}. \tag{6}$$

For matched conditions in the waveguide, (*i.e.*, $\Gamma_T = 0$) one gets $Z_{in} = -m_{22}/m_{21}$.

Eq. (5) gives us a direct hint on how to determine the elements of the m matrix. If Z_T can be made into a variable, known reactance X_T, Γ_{in} can be measured for different values of X_T, and the Γ_{in} values will fall on a circle in a Smith chart from which the m values can be determined. For a varactor, this variable reactance is already present, and its value can be determined as a function of bias voltage. Measurements have to be performed at low power levels to prevent appreciable nonlinearity, and one Γ_{in}-circle has to be plotted for each frequency of interest.

The determination of the m's from the measured Γ_{in}-values can be done in the following way:

$$\text{Set } X_T = -\frac{1}{\omega C} = -\frac{S}{\omega}. \tag{7}$$

Near the reverse breakdown point, X_T is very high. Let us assume it to be infinity, and denote the corresponding Γ_{in}-value Γ_∞. Close to forward breakdown X_T is small, and we call $\Gamma_{in} = \Gamma_0$ at this point. X_T values between these extremes, can be called X_1, X_2, $\cdots$ etc., giving $\Gamma_{in} = \Gamma_1$, Γ_2, $\cdots$. For a certain pair X_N, Γ_N, one obtains from (5)

$$m_{21}^2 = \frac{1}{2jX_N}\left[\frac{1}{\Gamma_N - \Gamma_\infty} - \frac{1}{\Gamma_0 - \Gamma_\infty}\right]. \tag{8}$$

If $X_T = 0$ and ∞ actually were obtained at the breakdown points, only one intermediate pair X_1, Γ_1 would be required. However, this is not really the case, but one gets rather close to the actual points Γ_0 and Γ_∞. By taking measurements at several intermediate points, and performing a trial and error adjustment along the circle of Γ_0 and Γ_∞ until all X_N, Γ_N pairs give equal values on m_{21}, one can eliminate this source of error, as well as possible large errors in some Γ_N.

With m_{21} determined, the other parameters can be written in terms of known numbers

$$m_{11} = \Gamma_\infty m_{21}$$
$$m_{12} = \Gamma_0 m_{22} = \frac{\Gamma_0}{2(\Gamma_0 - \Gamma_\infty)m_{21}}. \tag{9}$$

Introducing (9) in (5) and (6) gives

$$\Gamma_{in} = \Gamma_\infty - \frac{\Gamma_\infty - \Gamma_0}{1 - 2jX_T m_{21}^2(\Gamma_\infty - \Gamma_0)} \tag{10}$$

$$Z_{in} = \frac{1}{m_{21}^2(\Gamma_\infty - \Gamma_0)}\cdot\frac{1 - \Gamma_T\Gamma_0}{1 - \Gamma_T\Gamma_\infty}. \tag{11}$$

It is likely that the matrix introduced above will find other applications than those mentioned in the introduction. For example, the method for Q-measurements on varactors described by Houlding[1] is based on a theorem that can easily be proved using formulas (10) and (11).

The theorem states that if the two port between the waveguide input and the junction terminals is lossless, except for a series resistance (the spread resistance R_S) at one of these terminals, the normalized impedance ζ_{in} in the waveguide, when referred to a certain reference plane, has a constant real part. Further, when X_T changes with an amount ΔX_T, the change in the imaginary part of ζ_{in} is

$$\Delta \text{ Im } (\zeta_{in}) = k\cdot\Delta X_T \tag{12}$$

where

$$k = \frac{\text{Re } (\zeta_{in})}{R_S}.$$

Since R_S is the only lossy part of the circuit, $|\Gamma_\infty|$ must be unity, and we can always select a reference plane in the waveguide such that $\Gamma_\infty = +1$. Since $|\Gamma_{in}| \leq 1$, the circle in the Smith chart will then coincide with a "constant r" circle, and $\text{Re}(\zeta_{in})$ is constant. (*i.e.*, independent of X_T). From (10) one obtains

$$\zeta_{in} = \frac{1 + \Gamma_{in}}{1 - \Gamma_{in}} = \frac{1 + \Gamma_0}{1 - \Gamma_0} - 4jX_T m_{21}^2. \tag{13}$$

The assumptions also imply that if $|\Gamma_T| = 1$, $\text{Re}(Z_{in}) = R_S$, regardless of the phase of Γ_T. In particular, for $\Gamma_T = -1$, (11) gives

$$Z_{in} = \frac{1}{4}\,\frac{1 + \Gamma_0}{1 - \Gamma_0}\cdot\frac{1}{m_{21}^2}. \tag{14}$$

Since $\text{Re}(\zeta_{in})$ is independent of X_T, we conclude from (13) that m_{21}^2 is real, and that $\text{Re}(1+\Gamma_0)/(1-\Gamma_0)$ is positive. $\text{Re}(Z_{in})$ is also positive, so m_{21}^2 must be positive. Combining (13) and (14), we finally get

$$\zeta_{in} = 4m_{21}^2(R_S - jX_T) + j \text{ Im}\left(\frac{1 + \Gamma_0}{1 \quad \Gamma_0}\right). \tag{15}$$

Eq. (12) is obviously satisfied by (15), and the theorem is proved.

MATS E. VIGGH
TRG, Inc.
East Boston, Mass.

[1] N. Houlding, "Measurements of varactor quality," *Microwave J.*, vol. 3, pp. 40–45; January, 1960.